

Supplemental Information

**Semi-automated single-molecule microscopy
screening of fast-dissociating specific
antibodies directly from hybridoma cultures**

Takushi Miyoshi, Qianli Zhang, Takafumi Miyake, Shin Watanabe, Hiroe Ohnishi, Jiji Chen, Harshad D. Vishwasrao, Oisorjo Chakraborty, Inna A. Belyantseva, Benjamin J. Perrin, Hari Shroff, Thomas B. Friedman, Koichi Omori, and Naoki Watanabe

Supplemental Figures

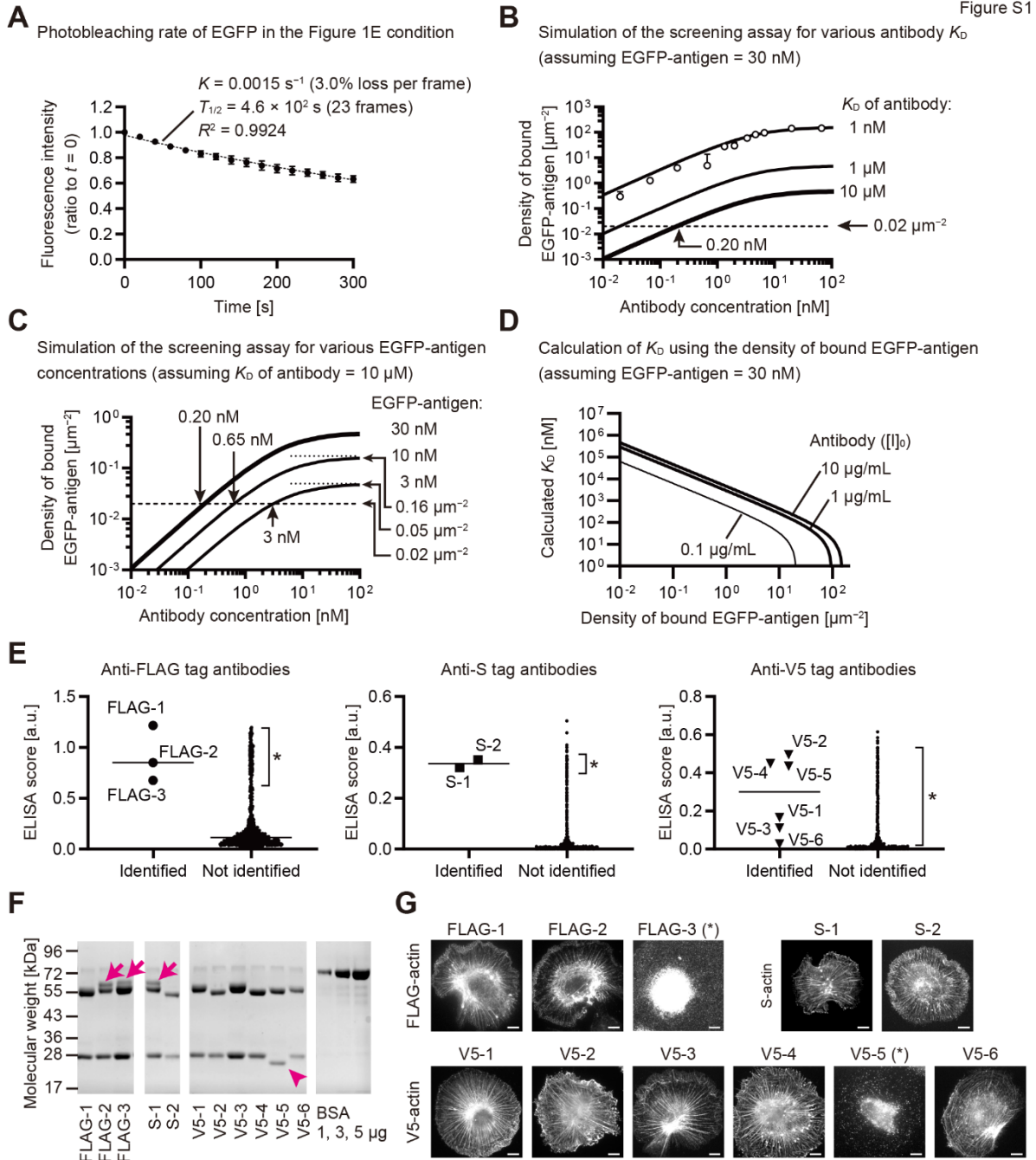


Figure S1, Related to Figures 1 and 2.

(A) Photobleaching rate of EGFP when acquired in the condition of Figure 1E (100 ms exposure every 20 s using the same laser power). EGFP was expressed as EGFP-actin in XTC cells, which was

weakly fixed and permeabilized to be immersed in HEPES-KCl-Tx buffer containing glucose, glucose oxidase and catalase as performed in the screening assay. Regression of fluorescence intensity was fit by a one-phase decay model to give a rate constant (K) = 0.0015 s⁻¹ (3.0 % loss per frame) and a half-life ($T_{1/2}$) = 4.6×10^2 s (23 frames). The 95% CIs were K = 0.00140 to 0.00158 s⁻¹ and $T_{1/2}$ = 4.37×10^2 to 4.94×10^2 s. Error bars, SDs (n = 3 cells). (B) The densities of bound EGFP-antigen in the screening assay were simulated to evaluate the sensitivity to antibodies with various affinities, K_D = 1 nM, 1 μ M and 10 μ M. Open circles are measured data between anti-V5 tag antibody and V5-EGFP in Figure 1D (error bars, SDs). Dashed line is the density of V5-EGFP bound to antibody-free glass surface, 0.02 spots/ μ m². An antibody with a K_D = 10 μ M is theoretically detected when applied at 0.20 nM, which corresponds to 0.030 μ g/mL assuming that the molecular weight of IgG is 150 kDa (Janeway et al., 2001), and is 30-fold lower than the typical antibody concentration in a hybridoma culture supernatant, 1–10 μ g/mL. (C) Simulation for a lower concentration of EGFP-antigen. Antibody of K_D = 10 μ M can be theoretically detected using 3 nM of EGFP-antigen when applied at 0.45 μ g/mL (3 nM), but the density of captured EGFP-antigen only elevates to 0.05 spots/ μ m² and are close to the density on antibody-free glass surface, 0.02 spots/ μ m². (D) K_D values calculated from the density of EGFP-antigen molecules assuming that antibodies were applied at 0.1, 1, and 10 μ g/mL (0.67, 6.7, and 67 nM). Calculated K_D was similar between 1 and 10 μ g/mL of antibody, which is the typical antibody concentration in hybridoma culture supernatants. Thus, the difference in the density of bound EGFP-antigen is considered to reflect the difference of K_D in this range of antibody concentration. The concentration of EGFP-antigen was set to 30 nM for this calculation. (E) ELISA scores of all anti-FLAG tag, anti-S tag, and anti-V5 tag candidates. The eleven antibodies identified in the screening (FLAG-1 to FLAG-3; S-1 and S-2; V5-1 to V5-6) did not show distinguishable ELISA scores. Many candidates showed scores similar to the identified antibodies (asterisks) although they did not show specific binding in the screening. Bars, medians. (F) SDS-PAGE analysis of identified anti-FLAG tag, anti-S tag, and anti-V5 tag antibodies. Antibodies in 1 mL culture supernatants were purified using Protein-A beads. The amounts of antibodies were quantified using BSA standards, ranging from 0.89 μ g (S-2) to 6.4 μ g (FLAG-3). FLAG-2, FLAG-3, and S-1 antibodies had extra bands in addition to the normal heavy chain bands around 55 kDa (arrows). The V5-5 antibody had a light chain of smaller size (~20 kDa; arrowhead), while other antibodies had normal chains around 25 kDa. (G) Conventional immunostaining of XTC cells expressing FLAG-actin, S-actin or V5-actin. Antibodies stained actin fibers via epitope tags except for FLAG-3 and V5-5 antibodies (asterisks). Bars, 10 μ m.

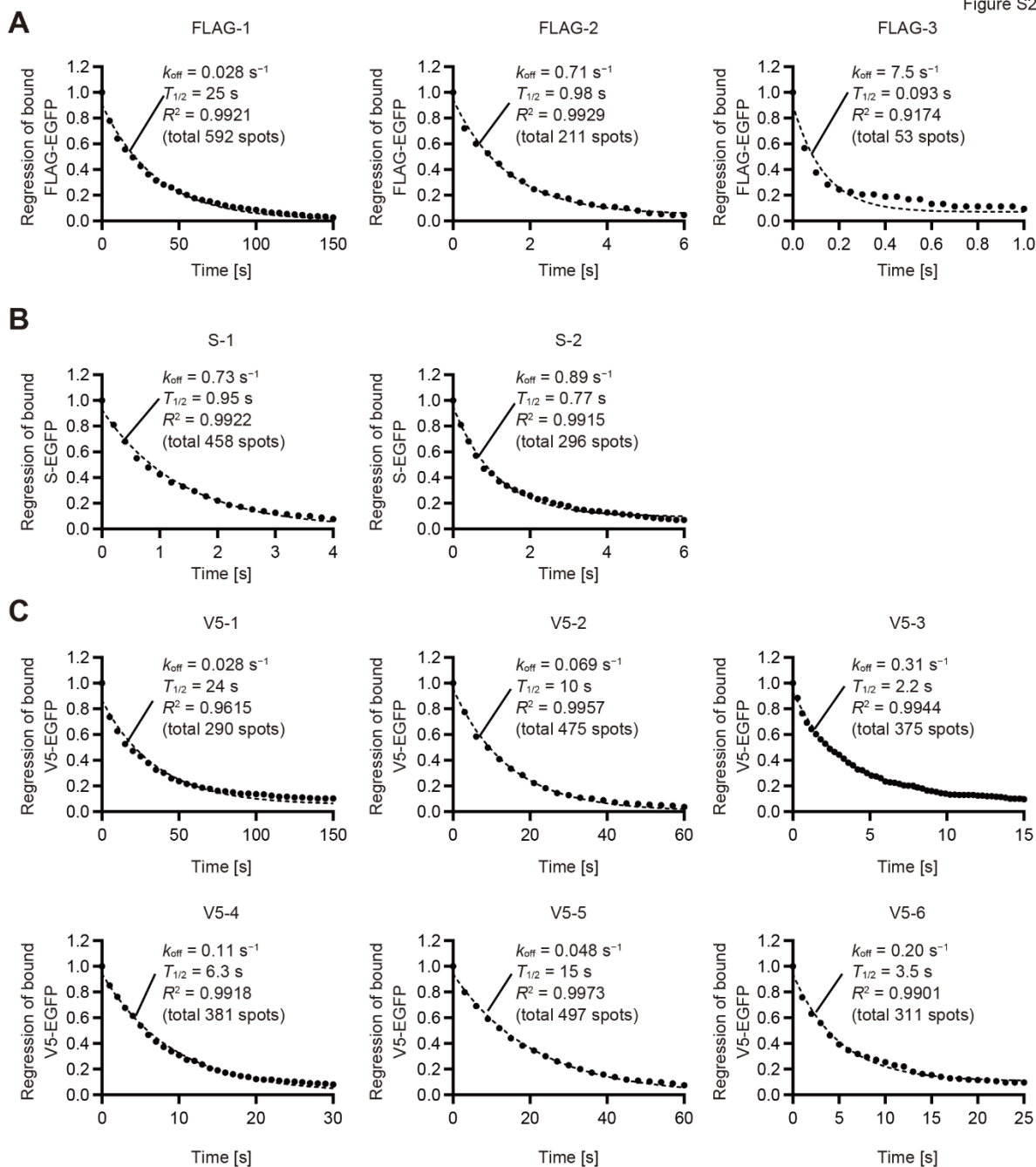


Figure S2, Related to Figure 3.

(A–C) The k_{off} of identified anti-FLAG tag, anti-S tag and anti-V5 tag antibodies determined from the regression of bound EGFP-antigen molecules (FLAG-EGFP, S-EGFP, and V5-EGFP) using the screening assay. Time-lapse images were acquired every 50 ms to 10 s to cause 10–30% exchange of bound EGFP-antigen molecules per frame. EGFP-antigens were diluted up to 0.1 nM to reduce the

density of bound EGFP-antigen molecules enough to distinguish each bound molecule. One-phase decay models were fit to the regression curves obtained from 53 to 592 molecules. See Table S2 for each k_{off} , $T_{1/2}$ and their 95% CIs. Exposure times were between 50 ms to 300 ms. The laser power was set to a similar level as in Figure 1E or set lower when possible.

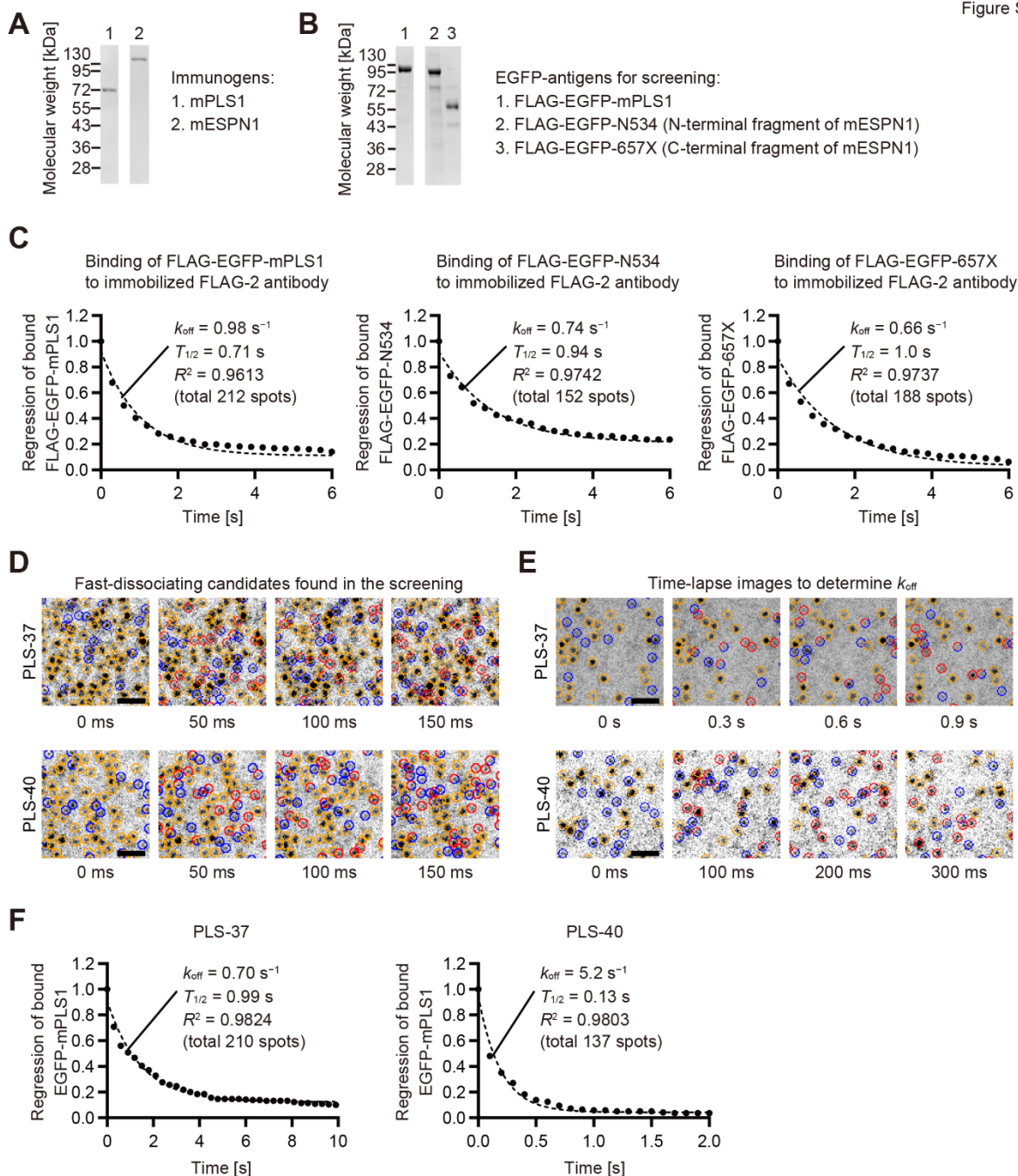


Figure S3, Related to Figure 4.

(A) SDS-PAGE of mPLS1 and mESPN1 recombinant proteins used to develop anti-mPLS1 and anti-mESPN1 antibodies. These proteins were synthesized in *E. coli*. (B) SDS-PAGE of EGFP-antigens used to screen anti-mPLS1 and anti-mESPN1 antibodies. These proteins were synthesized in HEK293 cells with FLAG tags for purification. FLAG-EGFP-mPLS1 is to screen anti-mPLS1

antibodies. FLAG-EGFP-N534 and FLAG-EGFP-657X are to screen anti-mESPN1 antibodies. These FLAG-EGFP-antigens were referred to as EGFP-mPLS1, EGFP-N534 and EGFP-657X in the main figures and in (D)–(F). (C) Regression curves of FLAG-EGFP-mPLS1, FLAG-EGFP-N534 and FLAG-EGFP-657X molecules bound to FLAG-2 antibody determined using the screening assay. Time-lapse images were acquired every 300 ms. k_{off} and $T_{1/2}$ were determined using one-phase decay models. The 95% CIs were $k_{\text{off}} = 0.856$ to 1.13 s^{-1} and $T_{1/2} = 0.616$ to 0.809 s for FLAG-EGFP-mPLS1; $k_{\text{off}} = 0.668$ to 0.820 s^{-1} and $T_{1/2} = 0.845$ to 1.04 s for FLAG-EGFP-N534; $k_{\text{off}} = 0.611$ to 0.717 s^{-1} and $T_{1/2} = 0.966$ to 1.13 s for FLAG-EGFP-657X. (D) Time-lapse images of fast-dissociating candidates during the screening. Representatively shown for PLS-37 and PLS-40 antibodies. Bound EGFP-mPLS1 molecules were frequently exchanged. Indication of circles is similar to Figure 1E. Time-lapse, every 50 ms. Bars, $2 \mu\text{m}$. (E) Time-lapse images of PLS-37 and PLS-40 antibodies used to determine k_{off} . The intervals of acquisition were adjusted to cause a 10–30% exchange of bound EGFP-mPLS1 per frame. Circles are the same as (D). Exposure times were 300 ms and 100 ms, respectively. The laser power was set to a similar level as in Figure 1E. Bars, $2 \mu\text{m}$. (F) Regression curves of EGFP-mPLS1 molecules bound to PLS-37 and PLS-40 antibodies determined using the time-lapse images in (E). k_{off} and $T_{1/2}$ were determined using one-phase decay models. The 95% CIs were $k_{\text{off}} = 0.624$ to 0.789 s^{-1} and $T_{1/2} = 0.878$ to 1.11 s for PLS-37; $k_{\text{off}} = 4.58$ to 5.98 s^{-1} and $T_{1/2} = 0.115$ to 0.151 s for PLS-40.

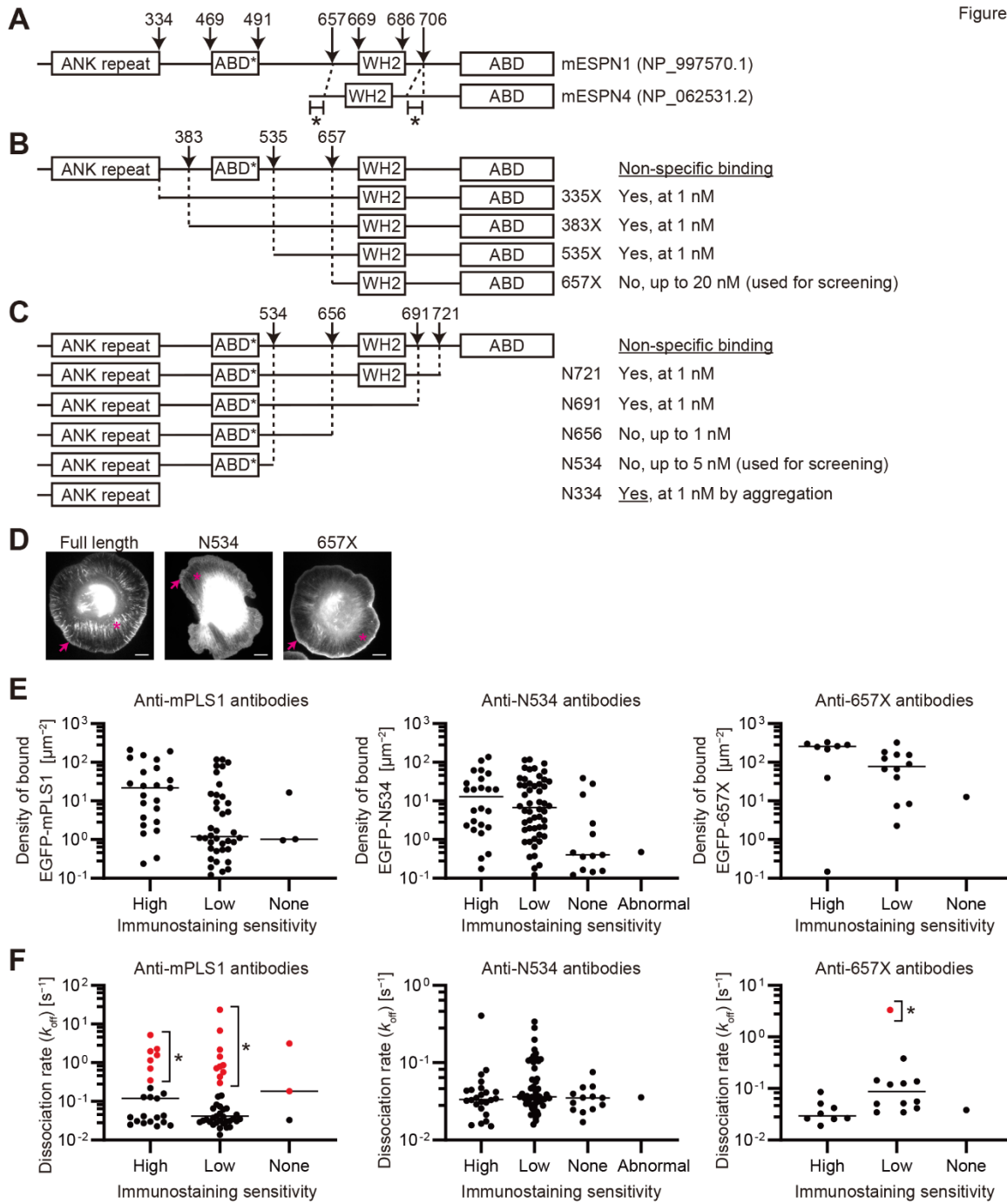


Figure S4, Related to Figure 4.

(A) Boundaries used to prepare EGFP-fused mESP1 (NP_997570.1) fragments. The 334th residue is the end of an ankyrin (ANK) repeat predicted using SMART (<http://smart.embl-heidelberg.de/>). The 669th to 686th residues are the WASP-Homology 2 (WH2) domain, which is followed by the

actin binding domain (ABD). The residues 469 and 491 include the 23 amino-acid sequence of the additional actin binding domain (ABD*) previously reported (Chen et al., 1999). The 657th residue is the beginning of the sequence present in the mouse espin 4 alternative splice isoform (mESPN4, NP_062531.2), which is the shortest isoform containing the ABD (asterisks are residues unique to mESPN4). (B) Preparation of C-terminal fragments. EGFP-fused fragments, 335X, 383X, 535X, and 657X, were applied on antibody-free glass surface. Non-specific binding was observed in EGFP-fused 335X, 383X, and 535X at 1 nM, but suppressed in EGFP-657X up to 20 nM. EGFP-657X was used for antibody screening at 20 nM. Confirmed by $n = 3$. (C) Preparation of N-terminal fragments. EGFP-fused N721 and N691 showed non-specific binding at 1 nM. Non-specific binding was suppressed in EGFP-N656 up to 1 nM and in EGFP-N534 up to 5 nM. The shorter fragment, EGFP-N334, bound to antibody-free glass surface due to aggregation. EGFP-N534 was used for antibody screening at 5 nM. From the result of (B) and (C), the residues, 535–656, were omitted to suppress non-specific binding. Confirmed by $n = 3$. (D) Intact functions of EGFP-fused mESPN1 full length, N534, and 657X expressed in XTC cells. Localization of all three EGFP-fused proteins in lamellipodia and filopodia (arrows) and in the abnormal thick filaments induced by these proteins (asterisks) indicates that actin binding activity was retained in N534 and 657X fragments. Bars, 10 μm . (E) Relationship between immunostaining sensitivity and affinity (the densities of bound EGFP-antigen molecules shown against the X-axes of Figures 4C and 4D). The affinity was compared among the antibodies showing “high sensitivity”, “low sensitivity”, “no staining” and “abnormal staining” in conventional immunostaining. The affinity is overlapped among the groups and not sufficient to predict immunostaining results. Bars, medians. (F) Relationship between immunostaining sensitivity and k_{off} (shown against the Y-axes of Figures 4C and 4D). Many fast-dissociating candidates recognized epitopes (red markers with asterisks). k_{off} values are overlapped among the groups and do not predict immunostaining results. Bars, medians.

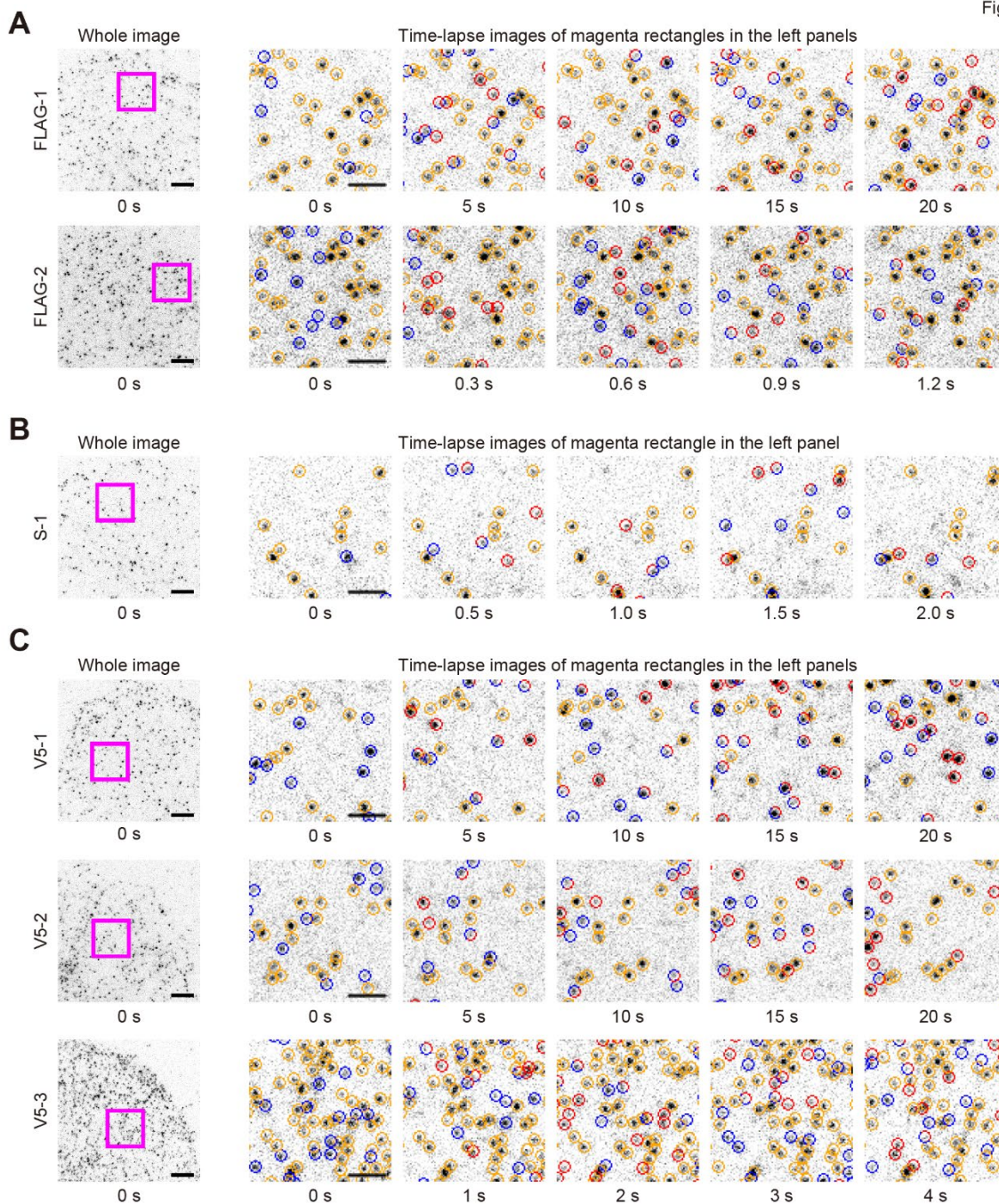


Figure S5, Related to Figure 5.

(A–C) Time-lapse images showing repetitive binding and dissociation of anti-epitope tag Fab probes that successfully recognized epitopes expressed in XTC cells. Fab probes were labeled with DyLight488 and applied at 0.1–1 nM onto XTC cells expressing FLAG-actin, S-actin, or V5-actin. The intervals of acquisition were adjusted to cause a 10–30% exchange of bound Fab probes per frame.

Indication of circles is similar to Figure 1E. Exposure, 300 ms for FLAG-2 and 50 ms for other Fab probes. Bars, 5 μm and 2 μm .

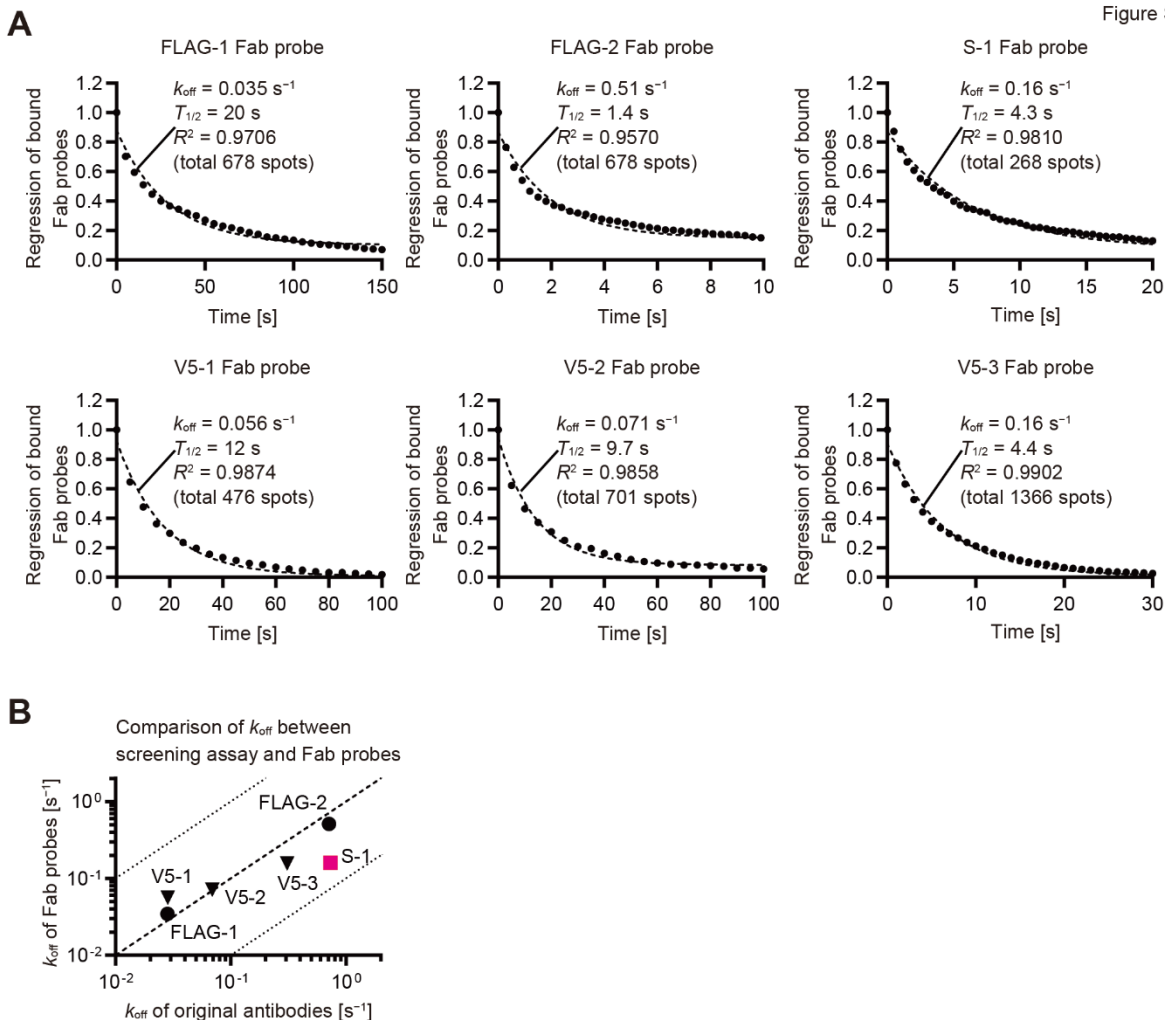


Figure S6, Related to Figure 5.

(A) k_{off} of anti-epitope tag Fab probes determined using the time-lapse images in Figure S5. To determine k_{off} and $T_{1/2}$, one-phase decay models were fit to the regression curves. The numbers of tracked Fab probe molecules were between 268 and 1,366. See Table S3 for each k_{off} , $T_{1/2}$ and their 95% CIs. (B) Comparison of k_{off} between Fab probes and original antibodies. k_{off} values of original antibodies were determined in Figure S2. Dashed line indicates equal k_{off} . Dotted lines indicate 10-fold faster or slower k_{off} . Anti-epitope tag Fab probes showed k_{off} similar to that of original antibodies except for S-1 Fab probe, which was 0.73 s^{-1} (half-life = 0.95 s) as antibody and 0.16 s^{-1} (half-life = 4.3 s) as Fab probe (magenta rectangle). See Tables S2 and S3 for each value.

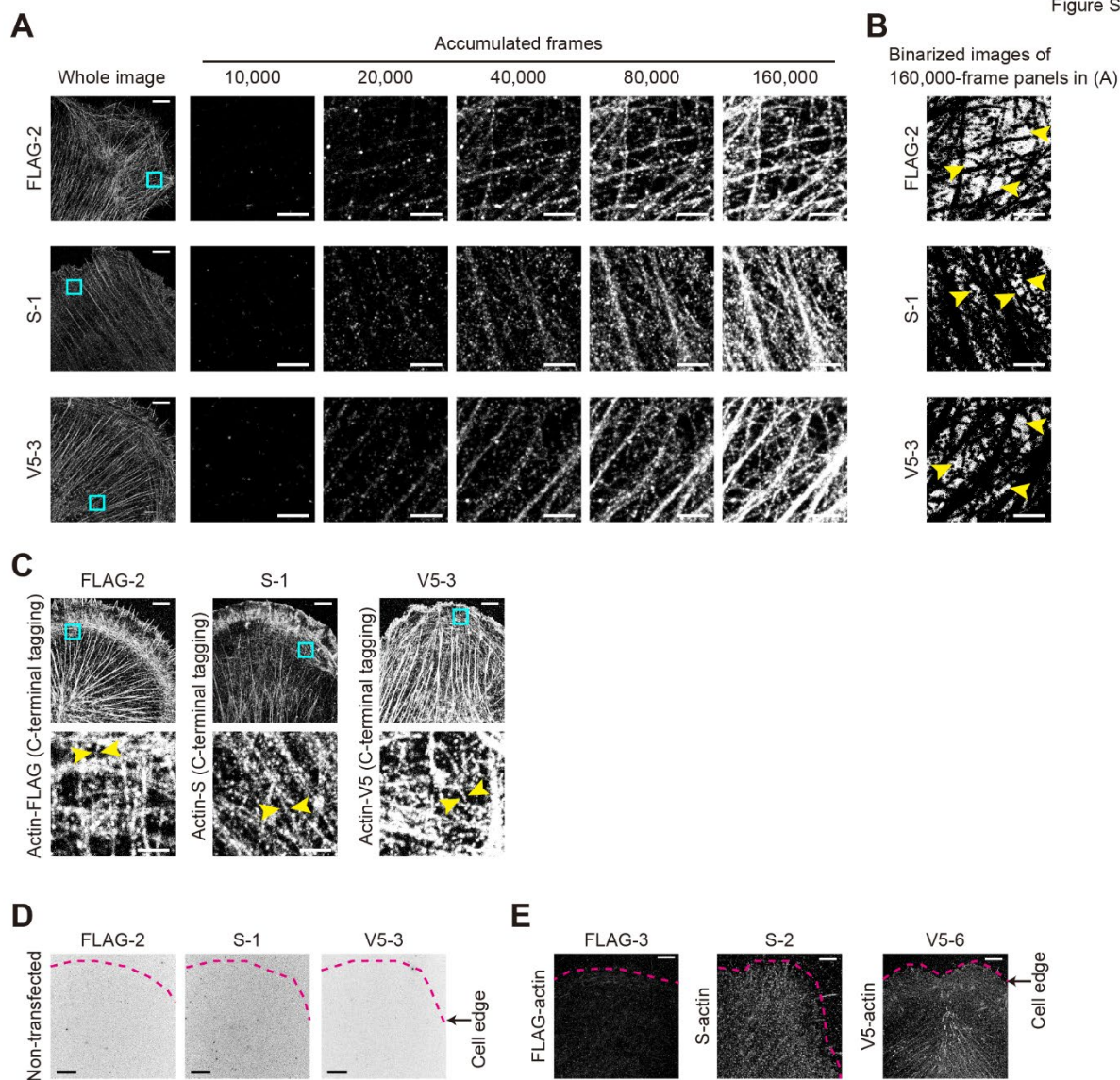


Figure S7, Related to Figure 5.

(A) Super-resolution images acquired with FLAG-2, S-1 and V5-3 Fab probes using XTC cells expressing FLAG-actin, S-actin and V5-actin, respectively. Reconstructed from 10,000, 20,000, 40,000, 80,000 and 160,000 frames. Whole image and the location of magnified images are identical to those in Figure 5. Thin actin fibers are visualized around 80,000 frames, but at higher densities at 160,000 frames. Bars, 5 μm and 2 μm . (B) Binarized images of 160,000-frame panels in (A) to confirm specific binding of FLAG-2, S-1 and V5-3 Fab probes. Images are reversed for black and white to show the area where Fab probes should not bind. Fab probes bound to actin fibers and

rarely bound to areas between fibers (arrowheads). Bars, 2 μm . (C) Super-resolution images acquired using XTC cells expressing actin fusing epitope tags at the C-terminus (actin-FLAG, actin-S and actin-V5). The FLAG-2, S-1 and V5-3 Fab probes were applied at 1 nM, respectively. Upper panels are the entire images, and the lower panels are magnification of cyan rectangles. Thin actin fibers were visualized by the frequent binding of these Fab probes (between arrowheads). Images are reconstructed from 160,000 frames acquired every 50 ms. Bars, 5 μm and 1 μm . (D) Binding of FLAG-2, S-1 and V5-3 Fab probes to non-transfected XTC cells. These Fab probes did not bind to XTC cells without epitopes. Images are maximum projections of 500 frames acquired every 50 ms. Fab probes, 1 nM. Bars, 5 μm . (E) Super-resolution images acquired with the Fab probes that did not show specific binding. Representatively shown for FLAG-3, S-2 and V5-6 Fab probes. Images were reconstructed from 40,000 frames acquired every 50 ms. Fab probes bound to the cells diffusely without visualizing actin fibers. Bars, 5 μm .

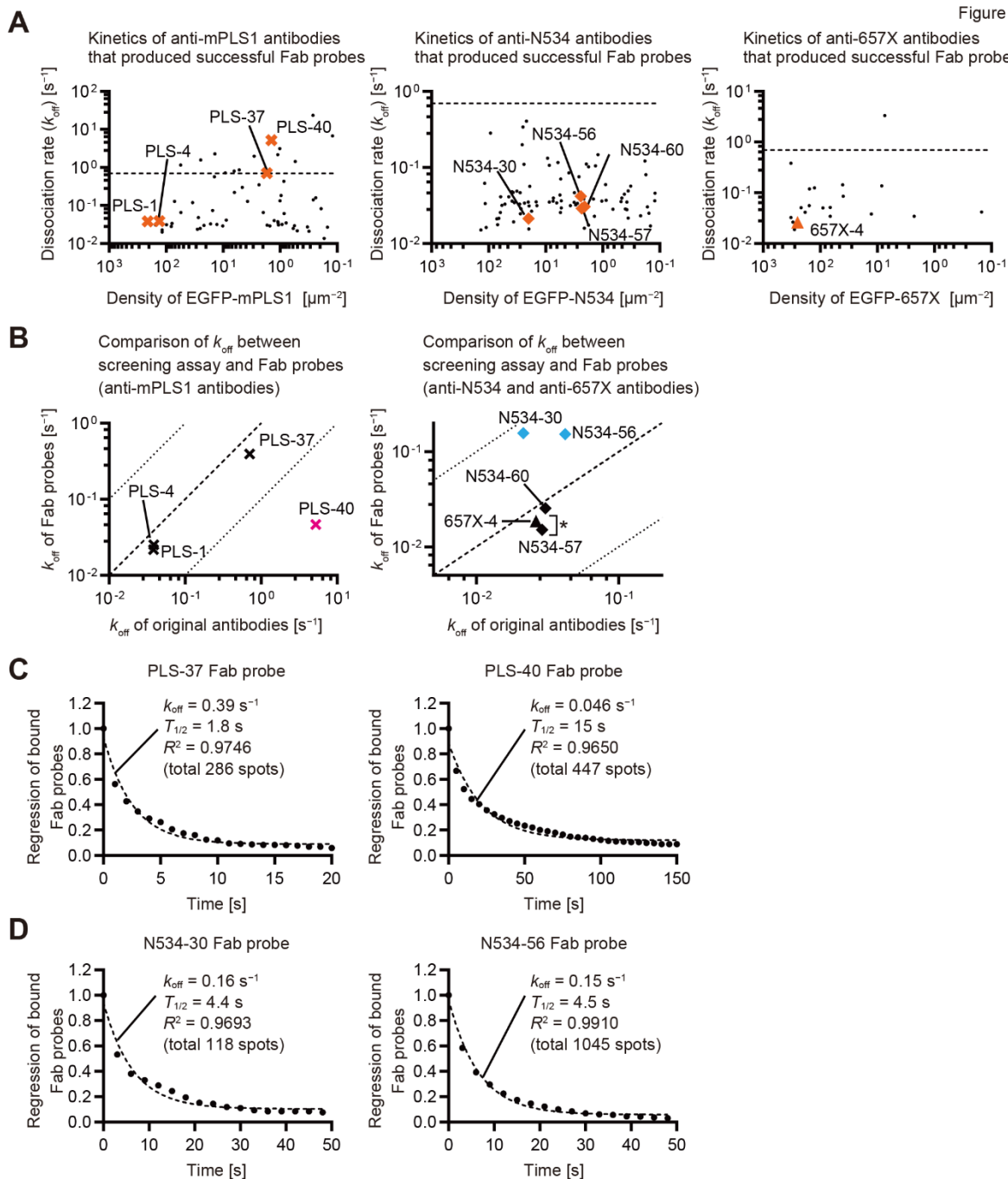


Figure S8, Related to Figure 6.

(A) Kinetics of anti-mPLS1 and anti-mESPN1 antibodies compared between antibodies that produced Fab probes with successful super-resolution imaging (orange crosses, diamonds and triangle) and antibodies that did not (black dots). k_{off} and the densities of bound EGFP-antigen are the values used in Figures 4C and 4D. These values are overlapped between antibodies of successful

imaging and non-successful imaging. Dashed lines indicate $k_{\text{off}} = 0.693 \text{ s}^{-1}$ (half-life = 1 s). (B) Comparison of k_{off} between Fab probes and original antibodies. k_{off} was determined from the regression of bound Fab probes. Dashed lines indicate equal k_{off} . Dotted lines indicate 10-fold faster or slower k_{off} . The k_{off} of PLS-40 anti-mPLS1 Fab probes was more than 10-fold slower than original antibodies (magenta cross). N534-30 and N534-56 Fab probes showed faster k_{off} than original antibodies (cyan diamonds). The k_{off} of N534-57 and 657X-4 Fab probes (asterisk) were the slowest among the five anti-mESPN1 Fab probes and may explain the low labeling density of these two Fab probes (Figures 6D and 6E). Representative regression curves are shown in (C) and (D). See Table S4 for each value. (C) Representative regression curves of PLS-37 and PLS-40 Fab probes shown to compare with Figure S3F. One-phase decay models were fit to the curves. The 95% CIs were $k_{\text{off}} = 0.321$ to 0.484 s^{-1} and $T_{1/2} = 1.43$ to 2.15 s for PLS-37 Fab probe; $k_{\text{off}} = 0.0381$ to 0.0564 s^{-1} and $T_{1/2} = 12.2$ to 18.1 s for PLS-40 Fab probe. Fab probes, 1 nM. (D) Representative regression curves of N534-30 and N534-56 Fab probes, which showed faster k_{off} than original antibodies. The 95% CIs were $k_{\text{off}} = 0.119$ to 0.206 s^{-1} and $T_{1/2} = 3.36$ to 5.80 s for N534-30 Fab probe; $k_{\text{off}} = 0.134$ to 0.174 s^{-1} and $T_{1/2} = 3.98$ to 5.19 s for N534-56 Fab probe. Fab probes, 1 nM.

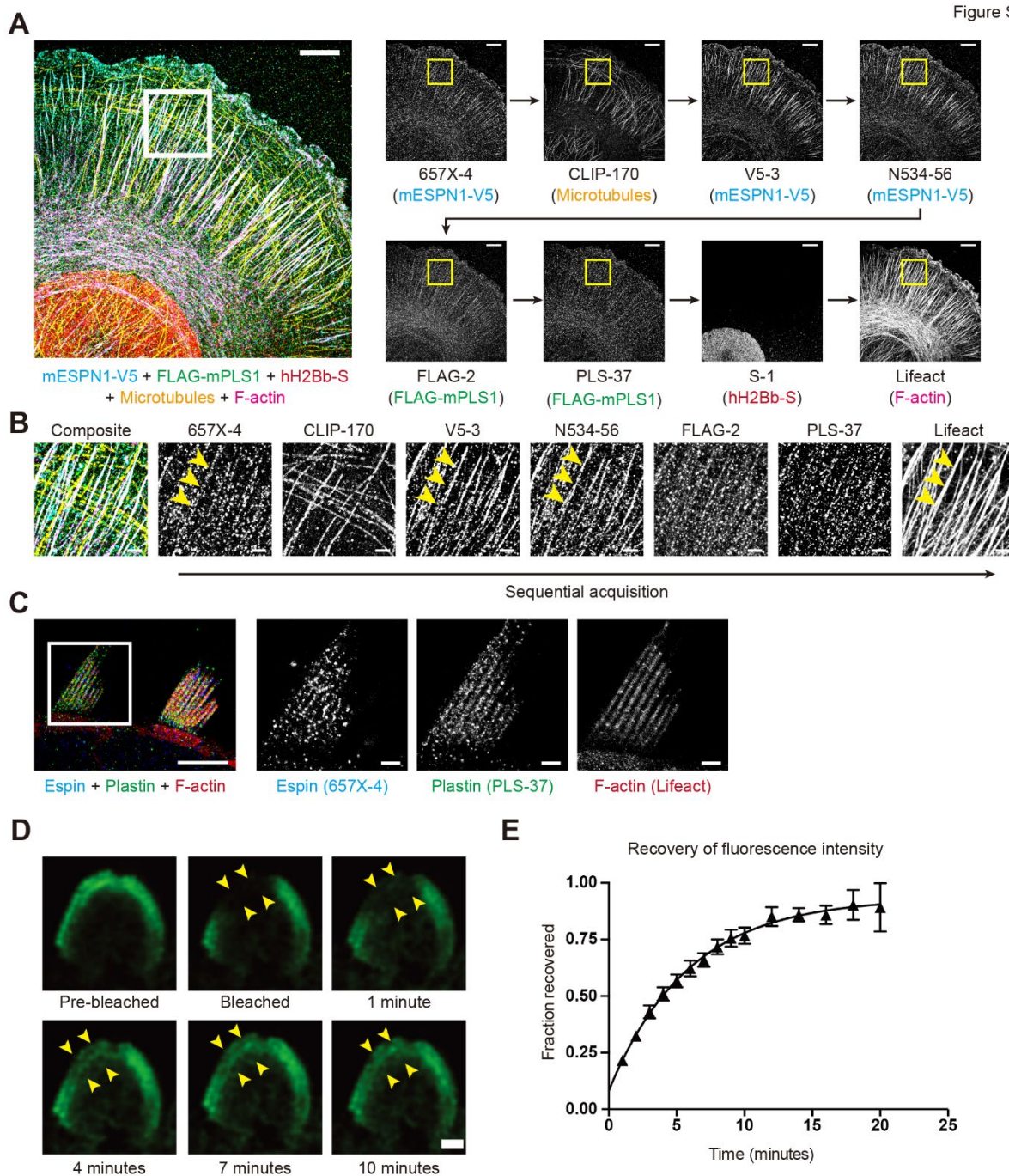


Figure S9, Related to Figure 7.

(A) Demonstration of probe substitutions by eight-color sequential imaging of XTC cells expressing mESP1-V5, FLAG-mPLS1, and hH2Bb-S (human histone cluster 1 H2B family member b with S tag). Super-resolution images were reconstructed from 50-ms time-lapse images acquired sequentially using six DyLight488-labeled Fab probes and two peptide-fragment probes (Atto488-

labeled Lifeact for F-actin and EGFP-fused CLIP-170 fragment for microtubules). The order of acquisition is 657X-4 (60,000 frames), CLIP-170 (20,000 frames), V5-3 (60,000 frames), N534-56 (60,000 frames), FLAG-2 (40,000 frames), PLS-37 (40,000 frames), S-1 (40,000 frames) and Lifeact (80,000 frames). The localization of bound probes was changed between 657X and CLIP-170; CLIP-170 and V5-3; N534-56 and FLAG-2; PLS-37 and S-1; and S-1 and Lifeact; consistent with the exchange of probes. Time-lapse images were acquired with TIRF illumination except for the S-1 probe (epi-illumination). Fab probes, 1 nM. Lifeact, 0.5 nM. CLIP-170, 1 nM. Bars, 5 μ m. (B) Magnified images of rectangles in (A). Only anti-mESPN1 and anti-V5 tag Fab probes visualized thick actin bundles induced by mESPN1 expression (arrowheads). Microtubules run independently. Bars, 1 μ m. (C) Imaging of endogenous espin and plastin. Frozen tissue sections (cryosections) of mouse vestibule (postnatal day 2) were imaged with 657X-4 and PLS-37 Fab probes. Counter-imaging used a Lifeact probe. Fab probes and Lifeact were labeled with DyLight550 and Atto550, respectively, to avoid green-spectrum autofluorescence of tissue samples. Time-lapse images were acquired every 200 ms for 40,000 frames using 657X-4 and PLS-37 Fab probes and every 50 ms for 80,000 frames using Lifeact. Fab probes, 1 nM. Lifeact, 0.5 nM. Bars, 5 μ m and 1 μ m. (D) FRAP experiment of EGFP-mESPN3a in outer hair cells (OHCs) from P3 mice. EGFP-mESPN3a in the stereocilia bundle was photobleached and imaged during recovery (arrowheads). Bar, 1 μ m. (E) Fluorescence recovery was quantified by measuring the fluorescence intensities of the bleached region of the cells normalized to those of the unbleached half of same cell at each time point (n = 4 cells from 3 separate experiments). Error bars represents SDs and the half-maximal recovery occurred at 3.9 minutes based on a non-linear curve that was fit to the data.

Supplemental Tables

Table S1, Related to Figure 2.

Antibody	Density of bound EGFP-antigen [μm^{-2}]	Fast-dissociating candidate? †	Epitope recognition in immunostaining ‡	Note
FLAG-1	$1.1 \times 10^2 \pm 2.8$ (*)	No	Success	
FLAG-2	0.93 ± 0.15	Yes	Success	
FLAG-3	0.084 ± 0.0020	Yes	Failed	
S-1	2.1 ± 0.052	Yes	Success	
S-2	1.0 ± 0.031	Yes	Success	
V5-1	44 ± 1.1 (*)	No	Success	
V5-2	7.4 ± 0.23 (*)	No	Success	
V5-3	6.0 ± 0.085 (*)	Yes	Success	
V5-4	5.1 ± 0.037 (*)	No	Success	
V5-5	3.2 ± 0.22 (*)	No	Failed	Truncated light chain
V5-6	0.98 ± 0.11	No	Success	

Values are means \pm SDs.

* Calculated using fluorescence intensity.

† Antibodies indicated as “Yes” showed frequent exchange of bound EGFP-antigen molecule in the screening assay.

‡ Tested using XTC cells expressing FLAG-actin, S-actin or V5-actin.

Table S2, Related to Figure 3.

Antibody	Dissociation rate (k_{off}) [s^{-1}]		Half-life [s]	
	Best fit value	95% CI	Best fit value	95% CI
FLAG-1	0.028	0.0272 to 0.0292	25	23.6 to 25.4
FLAG-2	0.71	0.634 to 0.790	0.98	0.876 to 1.09
FLAG-3	7.5 (*)	5.77 to 9.65	0.093 (*)	0.0718 to 0.120
S-1	0.73	0.711 to 0.751	0.95	0.921 to 0.978
S-2	0.89	0.820 to 0.968	0.77	0.715 to 0.844
V5-1	0.028	0.0259 to 0.0310	24	22.3 to 26.7
V5-2	0.069	0.0675 to 0.0711	10	9.74 to 10.2
V5-3	0.31	0.292 to 0.326	2.2	2.12 to 2.37
V5-4	0.11	0.105 to 0.113	6.3	6.09 to 6.56
V5-5	0.048	0.0468 to 0.0487	14.5	14.2 to 14.8
V5-6	0.20	0.178 to 0.219	3.5	3.16 to 3.88

* These fast dissociations may be an underestimate since the time-lapse images were acquired every 50 ms, which is the shortest interval possible in our system.

Table S3, Related to Figure 5.

Fab probe	Dissociation rate (k_{off}) [s^{-1}]		Half-life [s]	
	Best fit value	95% CI	Best fit value	95% CI
FLAG-1	0.035	0.0286 to 0.0413	20	16.7 to 24.2
FLAG-2	0.51	0.429 to 0.601	1.4	1.15 to 1.61
S-1	0.16 (*)	0.148 to 0.170	4.3 (*)	4.06 to 4.65
V5-1	0.056	0.0527 to 0.0598	12	11.5 to 13.1
V5-2	0.071	0.0614 to 0.0823	9.7	8.42 to 11.2
V5-3	0.16	0.150 to 0.164	4.4	4.22 to 4.62

* Slightly slower than those of original antibody.

Table S4, Related to Figure 6.

ID	In the screening assay		After conversion to Fab probes		
	k_{off} [s ⁻¹]	Half-life [s]	k_{off} [s ⁻¹]	Half-life [s]	
PLS-1	0.038	18	0.022	32	
PLS-4	0.039	18	0.025	28	
PLS-37	0.70	0.99	0.39	1.8	
PLS-40	5.2	0.13	0.046 (*)	15 (*)	
N534-30	0.021	32	0.16 (†)	4.4 (†)	
N534-56	0.042	17	0.15 (†)	4.5 (†)	
N534-57	0.029	24	0.015	46	
N534-60	0.031	23	0.025	28	
657X-4	0.026	26	0.019	36	

Best fit values are shown.

* 10-fold slower than those of original antibody.

† Nearly 10-fold faster than those of original antibodies.